Prospects for transferring $^{87}Rb^{84}Sr$ dimers to the rovibrational ground state based on calculated molecular structures

Tao Chen,[1,2] Shaobing Zhu,[1,2] Xiaolin Li,[1,*] Jun Qian,[1] and Yuzhu Wang[1,†]
[1]*Key Laboratory for Quantum Optics, Shanghai Institute of Optics and Fine Mechanics, Chinese Academy of Sciences, Shanghai 201800, China*
[2]*University of Chinese Academy of Sciences, Beijing 100049, China*
(Received 4 April 2014; published 4 June 2014)

Using fitted model potential curves of the ground and lowest three excited states yielded by the relativistic Kramers-restricted multireference configuration interaction method with 19 electrons correlated, we theoretically investigate the rovibrational properties including the number of vibrational state and diagonally distributed Franck-Condon factors for a $^{87}Rb^{84}Sr$ molecule. Benefiting from a turning point at about $v' = 20$ for the Franck-Condon factors between the ground state and spin-orbit $2(\Omega = 1/2)$ excited state, we choose $|2(\Omega = 1/2), v' = 21, J' = 1\rangle$ as the intermediate state in the three-level model to theoretically analyze the possibility of performing stimulated Raman adiabatic passage to transfer weakly bound RbSr molecules to the rovibrational ground state. With 1550 nm pump laser (2 W/cm^2) and 1342 nm dump laser (10 mW/cm^2) employed and appropriate settings of pulse time length (about 300 μs), we have formalistically achieved a round-trip transfer efficiency of 60%, namely 77% for one-way transfer. The results demonstrate the possibility of producing polar $^{87}Rb^{84}Sr$ molecules efficiently in a submicrokelvin regime, and further provide promising directions for future theoretical and experimental studies on alkali-alkaline(rare)-earth dimers.

DOI: 10.1103/PhysRevA.89.063402 PACS number(s): 37.10.Mn, 34.20.Cf, 33.20.Vq, 31.15.am

I. INTRODUCTION

Quantum sample of ultracold polar molecules [1], due to the tunable long-range and anisotropic interactions, not only provides access to many attractive new regimes in many-body physics [2–4] and ultracold chemistry [5], but also could be potentially applied in high-precision measurement [6,7], quantum computation, and quantum information processing [8,9]. During the past decade, formation, cooling, and trapping of molecules in a submicrokelvin regime have become a hot topic [10–16]. Since methods for direct cooling of molecules, such as buffer-gas cooling [11], Stark cooling [12], and optical cycling scheme [14], could only yield millikelvin samples, techniques including Feshbach resonance (FR) [17–20] and photoassociation (PA) [21–24] have been widely used in formation experiments of heteronuclear molecules from low-temperature precooled atom samples, mainly the alkali, alkaline-earth, and rare-earth metal atoms, to achieve lower temperature.

So far, polar molecules comprised of both alkali and alkaline(rare)-earth metal atoms mainly contain RbYb and LiYb dimers. The RbYb molecule has been created in the electronic ground state by two-color photoassociation and the PA spectroscopy has been measured simultaneously [25–27]. The scattering length studies and similar formation experiments for LiYb dimers are in exciting progress as well [19,28–32]. Even magnetic Feshbach resonances between the ground and ^3P metastable state of Yb have been observed [33] and an ultracold mixture of ground-state Li atoms and $^3P_2$ state Yb atoms has been realized recently [34]. However, the initially formed molecules are usually lying in high vibrational states and it is still difficult to produce a quantum degenerate molecule sample. As the stimulated Raman adiabatic passage (STIRAP) [35] has been performed to coherently transfer the formed KRb (a phase-space density of 0.1 order has been achieved by JILA group) [1,36,37], RbCs [38], and Cs_2 [39,40] molecules to the rovibrational ground state and even another transfer scheme with larger Franck-Condon factor (0.9474) for KRb has been proposed recently [41], coherent control of vibrational transfer [42] to create alkali-alkaline-earth dimers in a rovibrational ground state has become a new exciting direction to investigate at present.

Open-shell RbSr molecule has manifested good prospects in the ultracold physics field due to the electron spin in a rovibrational ground state and relatively large electric dipole moment [43], which allows convenient manipulations with external electric and magnetic field. Furthermore, laser cooling and trapping techniques for Rb and Sr have been well developed. The simultaneous magneto-optical trapping (MOT) [44], even double quantum degenerate samples (BEC) [45] of ^{87}Rb and ^{84}Sr, has been achieved experimentally. It is worth mentioning that Żuchowski *et al.* [46] have proposed a theoretical prediction of creating a $^{87}Rb^{84}Sr$ molecule with heteronuclear FR using the hyperfine structure of a Rb atom. The predicted background scattering length for $^{87}Rb^{84}Sr$ dimers can reach 1700 Å, and this is the most important issue to be demonstrated with the ongoing and future experiments. Another formation scheme using STIRAP has been mentioned in the creation experiment of Sr_2 molecules in the electronic ground state recently [47]. All of these make the formation of a $^{87}Rb^{84}Sr$ molecule become an anticipated matter. However, both of the formation approaches and the STIRAP require precise and systematic knowledge of molecular structures for a $^{87}Rb^{84}Sr$ dimer.

In this paper, efforts are focused on theoretical investigations of the electronic structures and rovibrational properties, mainly the Franck-Condon factors (FCFs) for the $^{87}Rb^{84}Sr$ molecule. Additionally, we briefly design a scheme to transfer the initial formed weakly bound molecules to the rovibrational

*xiaolin_li@siom.ac.cn
†yzwang@mail.shcnc.ac.cn

ground state. The article is organized as follows. In Sec. II, we present a detailed description of our *ab initio* relativistic calculations for the lowest four electronic states of a ^{87}Rb^{84}Sr molecule and the potential-energy curves are finally fitted with a model. Section III shows the procedure to obtain the eigenenergy series and wave functions by solving the radial Schrödinger equation numerically. The exact number of vibrational states supported by each potential curve is illustrated as well. The results are of particular importance for future spectroscopy experiments on the RbSr molecule. In Sec. IV we give a full scene of Franck-Condon factors for vibrational transitions from a rotationless ($J'' = 0$) ground state to the three excited states with $J' = 1$, and then theoretically investigate a similar STIRAP transfer process with that in Refs. [1,47] to confirm the possibility of creating the rovibrational ground state ^{87}Rb^{84}Sr molecules. Round-trip transfer efficiency of 60% is predicted by a generalized three-level model. Section V gives a conclusion for this work as well as an outlook for our future research on ultracold closed-shell–open-shell dimers.

II. ELECTRONIC STRUCTURE: RELATIVISTIC *AB INITIO* CALCULATION

A. *Ab initio* method

The *ab initio* electronic structure calculations for the ground state and low-lying excited states of the RbSr molecule are requisite to accessing the rovibrational information concerned. Since the rubidium atom and strontium atom are heavy with lots of electrons around the nuclei, the electron correlation and relativistic effect are significant and should be taken into consideration. For the excited states corresponding to the $[\mathrm{Rb}(5p^2P) + \mathrm{Sr}(5s^{21}S)]$ dissociation limit, the spin-orbit coupling (SOC) with states relevant to asymptote $[\mathrm{Rb}(5s^2S) + \mathrm{Sr}(5s5p^3P)]$ would be important because of the relatively small energy gap (about 1900 cm^{-1}) between the two asymptotes when compared with the D line transition ($5s^2S \rightarrow 5p^2P$) for ^{87}Rb (12579 cm^{-1} for $D1$ line and 12581 cm^{-1} for $D2$ line) and the energy difference (7200 cm^{-1}) between Sr $5s5p^3P$ and $5s5p^1P$ states.

Similar to previous calculation of the RbYb dimer [48], the relativistic Dirac-Coulomb Hamiltonian under a four-component framework has been chosen in our RbSr calculation to correctly describe the effect and spin-orbit coupling discussed above.

In terms of electron correlation, two approaches including the spin-restricted coupled-cluster method with single, double, and perturbative triple excitations [CCSD(T)] [46] and the configuration interaction by perturbation of a multiconfiguration wave function selected iteratively (CIPSI) method [43] were employed in previous studies of the RbSr ground state, which would serve as a benchmark for our calculations later. In this work, the calculations of both the ground and excited states are performed with relativistic Kramers-restricted multireference configuration interaction (KR-MRCI) with 19 electrons (Rb $4s^24p^65s^1$ and Sr $4s^24p^65s^2$) correlated. The number of correlated electrons is determined in the same way with the calculations of the Sr_2 molecule [49]. Previous studies on the RbYb system [26,27] have demonstrated that this approach can yield equilibrium distances and potential well depths for both ground and excited states in good agreement with experimental measurements. However, one thing that should be pointed out is that numerous correlated electrons result in a quite expensive requirement of calculation resource.

Molecular reference Kramers pairs for the configuration interaction program are obtained from Dirac-Coulomb Hartree-Fock (DCHF) self-consistent field calculation, in which an average of three valence electrons distributed in eight Kramers pairs including Rb $5s5p$ and Sr $5s5p$ spinors has been taken. Then the MRCI calculations take advantage of the concept of generalized active space (GAS) [50], which defines four active molecular orbital space subdivisions for RbSr. From the inside out, they are Rb $4s$ + Sr $4s$ spinors with four electrons, Rb $4p$ + Sr $4p$ spinors with at least 11 electrons in six Kramers pairs, Rb $5s5p$ + Sr $5s5p$ spinors with at least two electrons and at most three electrons in eight Kramers pairs, and finally all possible allowed single and double excitations in the remaining spinors space. All settings above are implemented in the DIRAC quantum chemistry program package [51].

Throughout the KR-MRCI calculation, Dyall's uncontracted aug-cc-pVTZ basis sets [53] for both Rb $(29s21p13d2f)$ and Sr $(29s21p13d3f)$ including the necessary $4s4p$ correlating and polarizing functions are applied. However, since we focus on the isotopes ^{87}Rb and ^{84}Sr, the Gaussian exponent for nuclear charge distribution used in the basis sets should be changed; otherwise, the basis sets could only be suitable for the most abundant isotopes ^{85}Rb and ^{88}Sr [54]. Although Angeli [55] provides a series of accurate nuclear charge radii through which the exponents could be yielded, we fulfilled the calculations with the standard Gaussian exponents ($2.299\,070\,265\,2 \times 10^8$ a.u. for ^{87}Rb and $2.346\,121\,327\,2 \times 10^8$ a.u. for ^{84}Sr) provided by Visscher and Dyall [56]. The basis set superposition error (BSSE) should be taken into account in calculations with large basis sets, which means the energy calculated in this work might need a counterpoise correction [57]. The BSSE can be determined with the following definition [58]: BSSE = $E^{A\{AB\}}(r) + E^{B\{AB\}}(r) - E^A - E^B$, in which $E^{A\{AB\}}(r)$ and $E^{B\{AB\}}(r)$ are monomer energies obtained by using the total basis $\{AB\}$ at the same geometry but with either A or B replaced by a ghost atom (when calculating atom A, the position of B is replaced; vice versa for B). For small basis sets, the BSSE usually can be daringly ignored. For rather large basis sets like that used for Yb, the BSSE are usually large at a magnitude of tens of cm^{-1} and thus need correction. For example, the value is about 20 cm^{-1} for the ground state of the RbYb system [48]. For a nearly symmetric diatomic system of RbSr, we have safely neglected the BSSE, since it has also been under no consideration in the calculation of the Sr_2 molecule [49]. In recent work on the RbSr system by Żuchowski *et al.* [59], they have not introduced the BSSE either which has been checked to be at the magnitude of less than 1 cm^{-1}. Energy change of such magnitude at every calculation point leads to little change of the fitting parameters of the model potential.

B. Model potential

To obtain the potential-energy curves (PECs) for the four lowest-lying electronic states represented by quantum number

TABLE I. Potential parameters of analytical fit for the ground state $1(\Omega = 1/2)$ and three lowest excited states of $^{87}Rb^{84}Sr$. The first column represents the spin-orbit molecular states described by quantum number $\Omega = \Lambda + \Sigma$.

Molecular state		r_e	ω_e	D_e	Long-range coefficients (a.u.)[a]		
Ω	$^{2S+1}\Lambda_{\Lambda+\Sigma}$	(a_0)	(cm^{-1})	(cm^{-1})	C_6	C_8	C_{10}
1(1/2)	$X^2\Sigma_{1/2}$	8.827	36.017	1017.58	3.699×10^3	4.609×10^5	5.833×10^7
2(1/2)	$1^2\Pi_{1/2} + 2^2\Sigma_{1/2}$	7.267	85.724	7883.09	1.753×10^4	4.431×10^6	9.625×10^8
1(3/2)	$1^2\Pi_{3/2}$	7.286	87.176	7957.31	8.331×10^3	5.681×10^5	4.460×10^7
3(1/2)	$2^2\Sigma_{1/2} + 1^2\Pi_{1/2}$	8.385	58.432	4683.56	8.331×10^3	5.681×10^5	4.460×10^7

[a]The coefficients data from Ref. [52].

Ω in Table I, the *ab initio* calculation has been implemented with different internuclear distances from $r = 3a_0$ to $r = 20a_0$. Then the PECs are fitted with the analytical form

$$V(r) = D_e[e^{-2\alpha(r-r_e)} - 2e^{-\alpha(r-r_e)}][1 - f(r)] - f(r)(C_6 r^{-6} + C_8 r^{-8} + C_{10} r^{-10}), \quad (1)$$

which is physically consistent at both short and long ranges. The Morse potential at short range is connected with the long-range analytical form by the switching function used in Ref. [60],

$$f(r) = \begin{cases} 0, & r \leqslant a, \\ \frac{1}{2} + \frac{1}{4}\sin\frac{\pi x}{2}\left(3 - \sin^2\frac{\pi x}{2}\right), & a < r < b, \\ 1, & r \geqslant b, \end{cases} \quad (2)$$

in which $x = [(r-a) + (r-b)]/(b-a)$. The switching range (a,b) is chosen as (6,12) Å by hand during the fit, and the long-range dispersion coefficients C_6, C_8, C_{10} are fixed with the values [52,61] in Table I. The parameters of Morse potential for the fitted model are also listed in Table I and the PECs are shown in Fig. 1.

The fit is necessary for two reasons. First, the calculated data is performed with a general fit to Morse potential at short range, which has been widely done in many previous works on different diatomic systems, to get the parameters including the potential depth and the equilibrium distance. Another reason is that subsequent numerical method in Sec. III takes a rather small numerical step and we need to know the potential even within one step. With the fit, we obtain knowledge of the potential information from the long range to the short range including the switching region. Since the Morse potential for diatomic molecule, the long-range potential form, and the switch function have all been demonstrated to be physically consistent, the results from this widely used potential form are trustworthy.

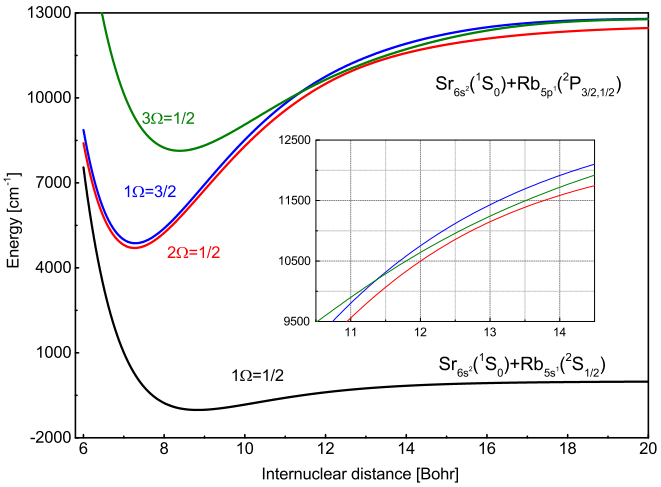

FIG. 1. (Color online) Spin-orbit potential-energy curves with the dissociation limits for ground state (black) and three lowest excited states of the $^{87}Rb^{84}Sr$ molecule. The inset figure is the PECs of the three excited states zoomed in from $10.5a_0$ to $14.5a_0$. A cross happens at about $11.5a_0$ and an avoided crossing at $13a_0$.

C. Results and comparison

The electronic ground state $1(\Omega = 1/2)$, mainly determined by the spin-free $X^2\Sigma_{1/2}$ state [the spin free here does not mean spinless; it is corresponding to the statement of the spin-orbit coupling $1(\Omega = 1/2)$ state], exhibits a very shallow potential depth of 1017.58 cm^{-1} (see Fig. 1), which is a universal character for the ground state of the Van der Waals molecule of alkali-alkaline(rare)-earth dimers [27,43,62,63]. The equilibrium distance we obtained is $r_e = 8.827a_0$. The result is in good agreement with another two works on the RbSr ground state as Żuchowski *et al.* [46] obtained a well depth of $D_e = 1000$ cm^{-1} with the equilibrium position at $8.86a_0$ and Guérout *et al.* [43] got $D_e = 1073$ cm^{-1} with $r_e = 8.69a_0$.

Similar to the RbYb molecule [48,64], an avoided crossing between the first excited state $2(\Omega = 1/2)$ and the third excited state $3(\Omega = 1/2)$ emerges at an internuclear distance of about $13a_0$, while the potential curves of the second excited state $2(\Omega = 3/2)$ and the third excited state cross each other at the position of about $11.5a_0$ (see the inset in Fig. 1).

The avoided crossing originates from the mixing of $1^2\Pi_{1/2}$ state and $2^2\Sigma_{1/2}$ state due to the strong spin-orbit coupling. Since the $2(\Omega = 1/2)$ state has the long-range character of $2^2\Sigma_{1/2}$ state, it should inherit the long-range dispersion coefficients of $2^2\Sigma_{1/2}$ state (see Table I) with dissociation limit $Sr(5s^2\,^1S_0) + Rb(5p^2P_{1/2})$.

In contrast with the $2(\Omega = 1/2)$ state, the third excited state $3(\Omega = 1/2)$ possesses the $2^2\Sigma_{1/2}$ state characters at short-range and long-range character of the $1^2\Pi_{1/2}$ state. For the $1(\Omega = 3/2)$ state, it shares the same dissociation limit $Sr(5s^2\,^1S_0) + Rb(5p^2P_{3/2})$ with the third excited state, but totally inherits the features of the $1^2\Pi_{3/2}$ state. Another important feature of the three excited states is that the equilibrium distances and the well depths of the $2(\Omega = 1/2)$ and $1(\Omega = 3/2)$ state are approximately the same (see Table I).

Recently, just as this work was nearly completed, Żuchowski *et al.* [59] reported a comparative study of the ground and excited states of RbSr molecule using both FCI/ECP + CPP and EOM-CCSD approaches, and they also discussed the transition dipole moment (TDM). Our results on the potential-well depths of the lowest four electronic states are approximately the same as their EOM-CCSD results and the discrepancy is less than 3%. For the equilibrium distance, we have the same value as that obtained from the EOM-CCSD method for the ground state, while a minor difference of $0.02a_0$ for excited states is found when compared with the values yielded by the FCI/ECP + CPP method in their work.

III. ROVIBRATIONAL PROPERTIES

Using the electronic structures attained in Sec. II, the eigenenergy and wave functions for the vibrational and rotational levels supported by the potential curves can be produced by solving the radial Schrödinger equation

$$-\frac{\hbar^2}{2\mu}\frac{d^2\psi}{dr^2}+\left[V(r)+\frac{\hbar^2}{2\mu r^2}[J(J+1)-\Omega^2]\right]\psi=E_{v,J}\psi, \tag{3}$$

in which μ is the reduced mass of the $^{87}Rb^{84}Sr$ molecule, $V(r)$ the electronic potential fitted in Eq. (1), and the second term behind $V(r)$ is the centrifugal potential of the diatomic molecule described by the rotational quantum number J and the axis projection of electronic angular momentum Ω.

A. Numerical methods

To obtain the rovibrational eigenenergy $E_{v,J}$, we begin with inserting a trial energy E_T in Eq. (3) to get the wave function, which is employed to perform a correction to the corresponding trial energy subsequently. The procedure is repeated by replacing the trial energy with the corrected energy until the corrected energy changes smaller than the criteria.

The trial energy series are generated with the near-dissociation theory [65]. Since a correction will be done later, the trial energy does not need to be too accurate. Here, the trial energies for the vibrational levels lower than $0.1D_e$ take the form of the approximate rotationless harmonic-oscillator solution: $E(v)=\omega_e(v+1/2)-\omega_e\chi_e(v+1/2)^2$, in which $\omega_e\chi_e=\omega_e^2/(4D_e)$ and v is the vibrational number, and the trial energies for the higher vibrational levels are generated with the recursive formula [65]

$$E_T(v)=D_e-[D_e-E_T(v-1)]\times\left[2-\left(\frac{D_e-E_T(v-2)}{D_e-E_T(v-1)}\right)^{1/p}\right]^p, \tag{4}$$

where $p=2n/(n-2)$ along with $n=10$ for long-range potential. All these trial energies contain no rotational terms which should be corrected.

Then we calculate the wave function corresponding to the trial energy numerically under the symplectic scheme [66]. Instead of using the B function in Ref. [67], we get

$$B(r,E,J)=\beta\left[E-V(r)-\frac{J(J+1)-\Omega^2}{\beta r^2}\right], \tag{5}$$

with $\beta=2\mu/\hbar^2$ by making a transformation of Eq. (3). We choose the numerical scale from $r_{\text{init}}=2a_0$ to $r_{\text{end}}=60a_0$, the step number $N=2\times10^4$, and as a result the step length $h=(r_{\text{init}}-r_{\text{end}})/N$.

Two-step second-order symplectic numerical procedure can be described by the following formula:

$$\begin{aligned}\phi(r_n)&=\psi(r_n)+h\varphi(r_n)/2,\\ \varphi(r_{n+1})&=\varphi(r_n)-h\phi(r_n)B(r_{n+1/2}),\\ \psi(r_n)&=\phi(r_n)+h\varphi(r_{n+1})/2,\end{aligned} \tag{6}$$

in which $\varphi(r)=d\psi(r)/dr$ and $r_n=r_{\text{init}}+nh$. For a specific rotational number J, this procedure can be performed either from the initial position with boundary condition $\psi(r_{\text{init}})=0$, $\varphi(r_{\text{init}})=1$ or from the final position with $\psi(r_{\text{end}})=0$, $\varphi(r_{\text{end}})=-1$. To improve the accuracy, one can maintain the four-step symplectic scheme [67] or just choose a larger step number, and the numerical scale might also be changed.

B. Energy correction

The eigenenergy correction follows the procedure already described in detail by Cooley and Cashion in Refs. [68,69]. For a trial energy given by Eq. (4), the numerical procedure above is employed to get the wave function $\psi_{\text{out}}(r_m)$ from the initial position out to the chosen matching point r_m, and $\psi_{\text{in}}(r_m)$ from the final position in to r_m. Here we choose $r_m=r_e$ (equilibrium position). Since the wave function should keep continuous at any position, $\psi(r_m)$ is forced to equal one and the discontinuous slopes of ψ_{out} and ψ_{in} at r_m are used to determine the energy correction

$$E_{\text{corr}}=\frac{[2-\psi_{\text{out}}(r_{m-1})-\psi_{\text{in}}(r_{m+1})]/h^2-B(r_m)}{\beta\left(\sum_{i=0}^{m}\psi_{\text{out}}^2(r_i)+\sum_{i=m+1}^{N}\psi_{\text{in}}^2(r_i)\right)}. \tag{7}$$

However, to avoid some undesired eigenenergies, since the energy gap between two adjacent vibrational levels should decrease monotonically or the corrected energy might have already occurred in the corrected series, we usually have to perform the correction again and again with different matching points r_m. In this work, r_m changes from $0.9r_e$ to $1.1r_e$ by step $0.01r_e$. Generally, the actual number of vibrational levels is much smaller than that of the trial energy series.

It can be concluded that the errors of the eigenenergies are mainly determined by the numerical step length h and the size of the numerical range. We do not give an analytical mathematical form for the error here; instead another two groups of eigenenergy data determined with different step length and end point of numerical range are presented in Table II. Making a comparison of the three groups, we have found that the eigenenergy values change with a maximum of only about 0.01 cm^{-1} when the end point changes from $60a_0$ to $100a_0$ with step length unchanged, while the eigenenergy values change at most about 0.1 cm^{-1} when we double the step length to $2h$ with the end point remains at $100a_0$. This is evidence that the errors of the eigenenergies are mainly determined by the step size.

For the uncertainty of the near-dissociation binding energy, we would like to take the ground state as an example to

TABLE II. Vibrational eigenenergy for the electronic ground state $1(\Omega = 1/2)$ with rotational number $J'' = 0$. The first column is the vibrational number; the subsequent three columns are the eigenenergies relative to the dissociation limit obtained with different numerical step length and numerical range. E_1 corresponding to end point at $60a_0$ with step number of 2×10^4, E_2 for end point at $100a_0$ with same step length with E_1, and E_3 for end point at $100a_0$ but double the step length to $2h$.

v''	E_1 (cm^{-1})	E_2 (cm^{-1})	E_3 (cm^{-1})	v''	E_1 (cm^{-1})	E_2 (cm^{-1})	E_3 (cm^{-1})
61	−0.09036	−0.09068	−0.09227	30	−210.742	−210.725	−210.851
60	−0.26368	−0.26325	−0.26648	29	−227.490	−227.473	−227.598
59	−0.57868	−0.57796	−0.58342	28	−244.905	−244.889	−245.012
58	−1.07887	−1.07777	−1.08603	27	−262.988	−262.971	−263.093
57	−1.80644	−1.80490	−1.81650	26	−281.737	−281.721	−281.840
56	−2.80213	−2.80007	−2.81552	25	−301.151	−301.136	−301.252
55	−4.10442	−4.10178	−4.12155	24	−321.230	−321.215	−321.328
54	−5.74842	−5.74515	−5.76962	23	−341.971	−341.957	−342.066
53	−7.76543	−7.76141	−7.79088	22	−363.374	−363.360	−363.464
52	−10.1764	−10.1718	−10.2064	21	−385.435	−385.422	−385.522
51	−12.9913	−12.9860	−13.0257	20	−408.153	−408.141	−408.236
50	−16.2236	−16.2176	−16.2625	19	−431.527	−431.515	−431.605
49	−19.9027	−19.8960	−19.9464	18	−455.555	−455.544	−455.628
48	−24.0743	−24.0668	−24.1232	17	−480.235	−480.225	−480.303
47	−28.7931	−28.7847	−28.8476	16	−505.567	−505.558	−505.630
46	−34.1115	−34.1021	−34.1719	15	−531.551	−531.542	−531.609
45	−40.0706	−40.0603	−40.1370	14	−558.185	−558.177	−558.238
44	−46.6971	−46.6860	−46.7694	13	−585.471	−585.464	−585.518
43	−54.0053	−53.9933	−54.0831	12	−613.408	−613.402	−613.450
42	−62.0003	−61.9875	−62.0833	11	−641.997	−641.991	−642.034
41	−70.6821	−70.6685	−70.7699	10	−671.236	−671.231	−671.268
40	−80.0480	−80.0338	−80.1402	9	−701.127	−701.123	−701.155
39	−90.0945	−90.0797	−90.1905	8	−731.670	−731.666	−731.693
38	−100.818	−100.803	−100.917	7	−762.864	−762.861	−762.882
37	−112.215	−112.200	−112.318	6	−794.709	−794.707	−794.723
36	−124.284	−124.268	−124.389	5	−827.206	−827.204	−827.216
35	−137.023	−137.006	−137.130	4	−860.354	−860.353	−860.361
34	−150.430	−150.414	−150.538	3	−894.154	−894.153	−894.159
33	−164.506	−164.489	−164.615	2	−928.605	−928.605	−928.608
32	−179.250	−179.233	−179.360	1	−963.708	−963.708	−963.709
31	−194.662	−194.645	−194.772	0	−999.463	−999.463	−999.463

provide some warnings here. In fact, the potential at the point of $60a_0$ is $-0.018\ cm^{-1}$ below the dissociation limit, which means it is reasonable to assume the wave function at $60a_0$ being zero for almost all the vibrational levels except several higher near-dissociation levels, since the end point of $60a_0$ lies in the classically forbidden region within which the wave function dies off exponentially. One should resort to a rather large numerical range (the end point at position of thousands of a_0) to reduce the uncertainty for the near-dissociation levels.

C. Number of vibrational states

For the $^{87}Rb^{84}Sr$ molecule, we focus on the electronic ground state with rotational number $J = 0$ and the three excited states with $J = 1$. Using the corrected eigenenergy series, the wave function for a specific vibrational level can be easily obtained with Eq. (6). Figure 2 shows the wave functions corresponding to the vibrational ground state briefly described as $|g, v'' = 0, J'' = 0\rangle$, the state $|g, v'' = 4, J'' = 0\rangle$, and the highest bound state $|g, v'' = 61, J'' = 0\rangle$ in a normalized potential well of the electronic ground state. It can be concluded that the wave functions for lower vibrational states are restricted near the equilibrium position while the bound states near the dissociation limit tend to dissociate easily due to large amplitudes of their wave functions within the long range.

For the rotationless ($J = 0$) ground state, as listed in Table II, we have conservatively concluded that there are 62 vibrational states lying below the dissociation limit. And the vibrational state numbers of 195, 189, and 149 are respectively supported by the PECs corresponding to $2(\Omega = 1/2)$, $1(\Omega = 3/2)$, and $3(\Omega = 1/2)$ excited states.

However, the actual number of the vibrational levels supported by the potential curves will finally be determined by future high-resolution two-color photoassociation spectroscopy in the same way as performed in experiments for RbYb [26] and Sr_2 [70] molecules, and thus the potential curves can be determined by the least-squares fitting procedure in Ref. [27]. As detailed investigations of the hyperfine and rovibrational structures of the $a^3\Sigma_u^+$ state of $^{87}Rb_2$ have already been done with high-resolution two-photon dark-state spectroscopy [71], the data and methods in this section make excellent guidance for future experimental studies on the molecular structures for RbSr.

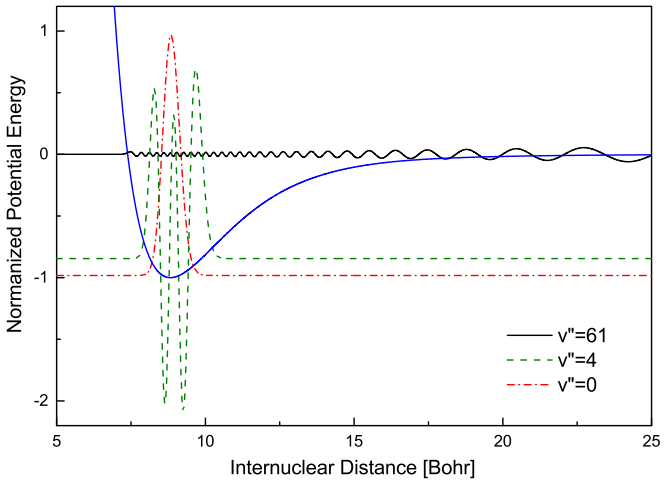

FIG. 2. (Color online) Wave functions for $v'' = 0$ (red), $v'' = 4$ (green), and $v'' = 61$ (black) supported by the electronic ground-state potential well (blue) with the depth normalized to 1.

IV. STIRAP TRANSFER SCHEME EXPLORATION

In this section, we show an overview picture of Franck-Condon factors for all transitions between the vibrational states in electronic ground state and the vibrational states in the three electronic excited states of a ^{87}Rb^{84}Sr dimer. Then a transfer scheme is investigated to yield the rovibrational ground-state ^{87}Rb^{84}Sr molecules. The transfer efficiency is estimated with a general three-level model.

A. Franck-Condon overlap

The Franck-Condon factor illustrated by the formula $f_{v''\to v} = |\langle g,v'',J''|e,v',J'\rangle|^2$ is calculated from the wave functions obtained in Sec. III. Since $J'' = 0 \to J' = 0$ transitions are dipole moment forbidden, the FCFs are calculated with $J'' = 0 \to J' = 1$ transitions, that is, R transition branch in the rotational spectroscopy. Figure 3 shows the full scene of the FCFs. For the $2(\Omega = 1/2)$ and $1(\Omega = 3/2)$ excited states, the factors for the vibrational transitions with electronic ground state $1(\Omega = 1/2)$ exhibit the same character with a turning point at position near $v' = 20$, which can be made out clearly in Figs. 3(a) and 3(b). It is worth mentioning that the turning point is a physical certainty, since it originates from the different equilibrium distance for the ground state and excited state.

Due to the character (nearly the same equilibrium distance with the electronic ground state $X^2\Sigma_{1/2}$; see Table I) of $2^2\Sigma_{1/2}$ state at short range for the $3(\Omega = 1/2)$ electronic excited states, the FCFs are largely diagonal without a turning point. Meanwhile, there is a branch from $v' = 0$ to $v' = 15$ above the diagonal, as illustrated in Fig. 3(c). The branch can be used to perform coherent transfer to lower vibrational states [72] and the diagonal FCFs are necessary to fulfill the STIRAP process efficiently.

Another important feature of the factors for $3(\Omega = 1/2)$ state is that the values can reach about 0.3 for the transitions between the several lowest-lying vibrational levels [see lower left corner of Fig. 3(c)], which may lead to a similar transfer scheme reported recently by Tokyo group for KRb molecule using $|b^3\Pi_0, v' = 0\rangle$ state [41].

B. Intermediate state

As pointed out by Ni *et al.* [1] in transferring the Feshbach KRb molecule to rovibrational ground state and by Aikawa *et al.* [37] for the photoassociated KRb molecule, it is of significant importance to select an intermediate state $|i\rangle$ in electronic excited states to couple both the initial formed molecule $|m\rangle$ and the final rovibrational ground state $|g,0,0\rangle$ with non-neglectable FCFs. Considering that smaller FCFs always lead to the requirement of much larger laser intensity, here we use a selection criterion function $F(m,i) = f_{m\to i} \times f_{i\to g,0,0}$ to determine the $|i\rangle$ state.

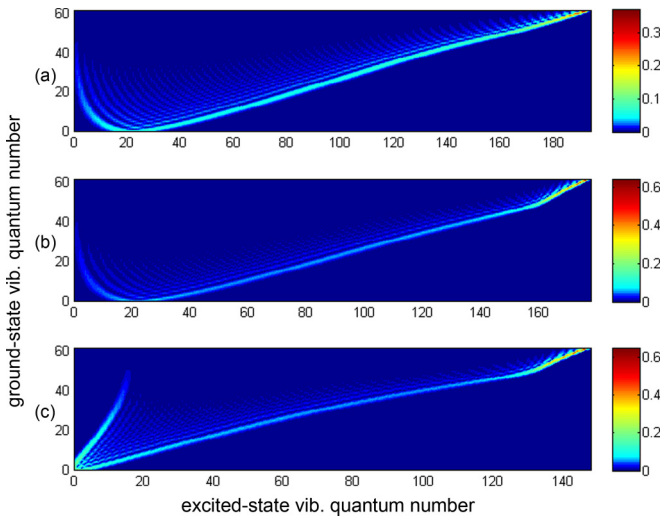

FIG. 3. (Color online) Franck-Condon factors as functions of the vibrational quantum numbers of the ground (vertical axis) and excited (horizontal axis) states. (a), (b), and (c) are respectively corresponding to the $2(\Omega = 1/2)$, $1(\Omega = 3/2)$, and $3(\Omega = 1/2)$ excited state.

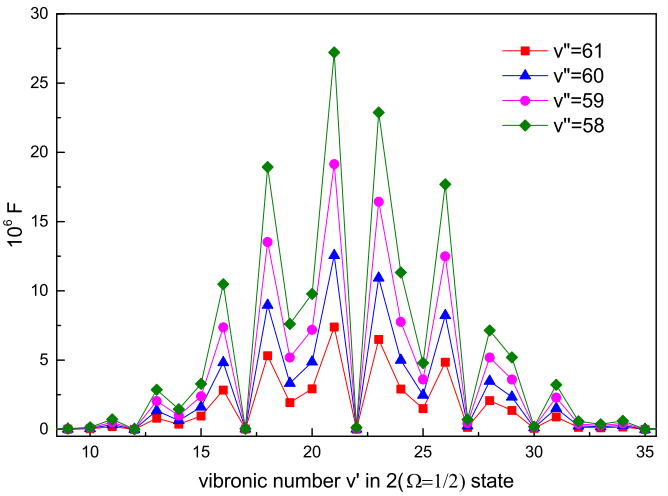

FIG. 4. (Color online) Series of F values corresponding to the intermediate $|i\rangle$ state number for the initial $|m\rangle$ state lying in the highest five vibrational levels in ground state (v'' number changes from 61 to 58).

For the initially formed weakly bound molecules, the initial $|m\rangle$ state lies in the higher several vibrational states in electronic ground state. Due to the highly diagonal distribution of FCFs for the vibrational states in $3(\Omega = 1/2)$ state, the F values are quite small (about 10^{-8} magnitude). However, for the $2(\Omega = 1/2)$ and $1(\Omega = 3/2)$ states whose FCFs behave in the same way, the F value can reach about 10^{-5} magnitude around the turning point and thus both of them can be used to perform the STIRAP. We take the $2(\Omega = 1/2)$ state as an example.

Figure 4 shows a series of F values corresponding to v from 10 to 35 in the $2(\Omega = 1/2)$ state. For different near-dissociation vibrational states $|m\rangle$ in the electronic ground state, the $v' = 18$, $v' = 21$, and $v' = 23$ states always have larger F value. To determine which vibrational state could be used as the $|i\rangle$ state, a search process can be performed experimentally by using the same method in the transfer experiments of KRb [1] or RbCs [38]. Here we choose $v' = 21$ as the intermediate state with reasonable Franck-Condon factors $f_{m\to i} = 3 \times 10^{-4}$ and $f_{i\to g,0,0} = 0.0935$. Since the intermediate state is deeply bound, the change caused by the numerical method and BSSE is not large enough to make a modification to the deeply bound vibrational state number.

C. Transfer scheme and efficiency

The transfer scheme involves three rovibrational states [see Fig. 5(a)]: the initial state $|m\rangle$, the intermediate state $|i\rangle$ ($|2(\Omega = 1/2), v' = 21, J' = 1\rangle$), and the final state $|g, v'' = 0, J'' = 0\rangle$. They are coupled by pump laser $L1$ and dump laser $L2$. The first laser pulse $L1$ (1549.5 nm) makes the weakly bound molecule state $|m\rangle$ transfer up to a deeply bound state $|i\rangle$ by overlapping the wave functions of the two states propitiously at the Condon point. The second laser pulse $L2$ (1341.8 nm) drives the molecules down to the rovibrational ground state $|g,0,0\rangle$ from the $|i\rangle$ state. The wavelengths of 1549.5 nm and 1341.8 nm are determined by the eigenenergy separations between the intermediate state $|i\rangle$ and the other two states ($|m\rangle$ and $|g,0,0\rangle$) mentioned above.

The intensity of the two laser pluses evolves in totally opposite tendency [see Fig. 5(b)]. The laser pulse $L2$ is switched on first and then drops off to nearly zero intensity in the shape of the Gaussian within time t_p, while the $L1$ pulse simultaneously ramps up from zero intensity to maximum value. After a hold time t_h(1 ms), a reverse mirror image of previous pulse is performed to measure the molecule number and efficiency. The pulse time t_p usually takes hundreds of microseconds [72,73].

To estimate the transfer efficiency, we employ a three-level model [74] to analyze the transfer process quantitatively. The model describes the dynamic evolutions of the quantum probability amplitudes C_m, C_i, and C_g respectively corresponding to states $|m\rangle$, $|i\rangle$, and $|g,0,0\rangle$ in the following formulas:

$$
\begin{aligned}
i\dot{C}_m &= -i\Gamma_m C_m/2 - \Omega_1 C_i/2,\\
i\dot{C}_i &= (\Delta_1 - i\Gamma_i/2)C_i - (\Omega_1 C_m + \Omega_2 C_g)/2,\\
i\dot{C}_g &= (\Delta_1 - \Delta_2 - i\Gamma_g/2)C_g - \Omega_2 C_i/2,
\end{aligned}
\tag{8}
$$

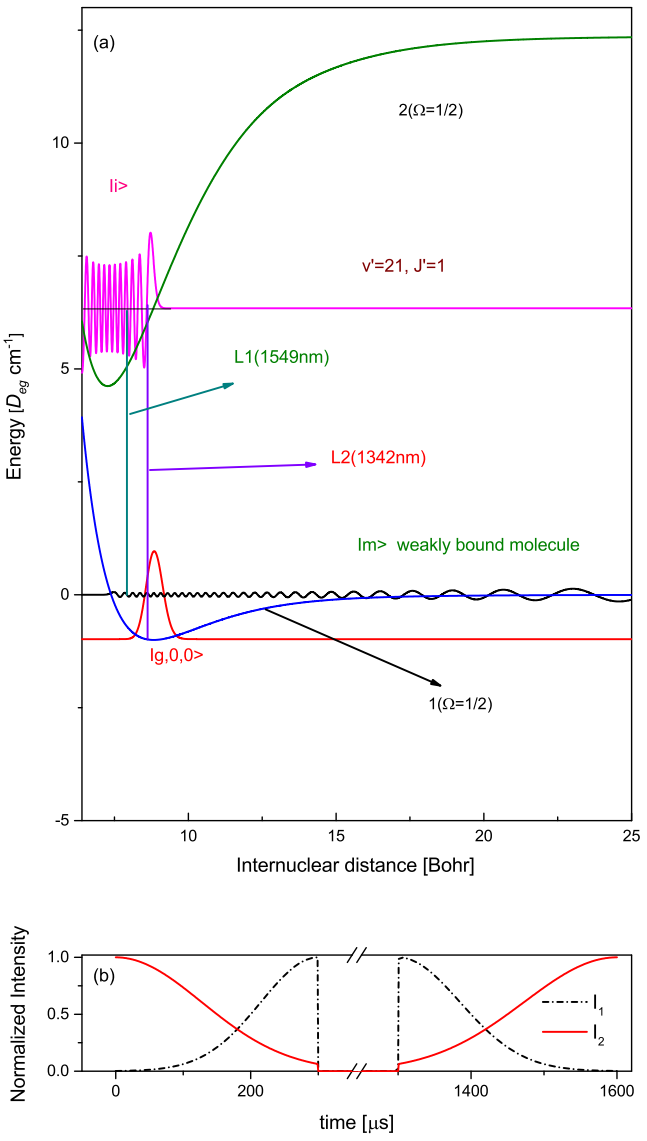

FIG. 5. (Color online) (a) STIRAP scheme for transferring the weakly bound molecule $|m\rangle$ to the rovibrational ground state via the intermediate state $|i\rangle$ lying in $2(\Omega = 1/2)$ state. The potential energies are divided by the ground-state well depth D_{eg}. (b) Evolutions of the intensity (normalized) of two STIRAP laser pulses (Gaussian shape). I_1 (black) for laser pulse $L1$ and I_2 (red) for laser pulse $L2$. The break between the association pulse (from 0 μs to 300 μs) and dissociation pulse (from 1300 μs to 1600 μs) represents the hold time (1 ms) during which two lasers are both turned off.

in which the Rabi frequency Ω and the decay rate Γ should be determined experimentally with the methods used in experiments for Sr_2 [47,75], Cs_2 [39,40], and Rb_2 [72,73] molecules. Here we take the Rabi frequency $\Omega = 2\pi \times 24.6\sqrt{f \times I}$MHz/(W/cm^2)$^{1/2}$ estimated with the transition dipole moment at equilibrium distance of the electronic ground state since the two Condon points are near the equilibrium distance (see Fig. 5), and the decay rate $\Gamma_i = 2\pi \times 6$ MHz, $\Gamma_m = 2\pi \times 0.5 I_2$ kHz/(W/cm^2), and $\Gamma_g = 2\pi \times 0.1 I_1$kHz/(W/cm^2) [72]. I_1 and I_2 are the pulse intensities (W/cm^2) with respect to $L1$ and $L2$. Since the lasers

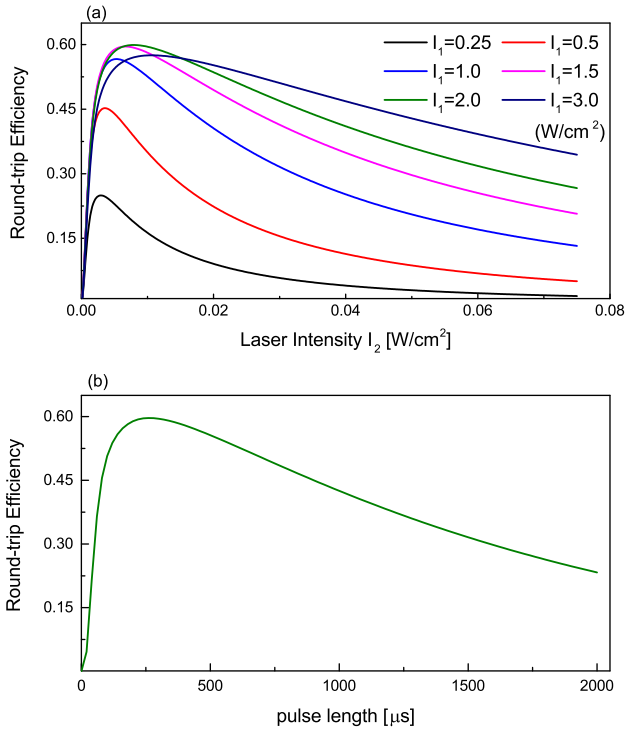

FIG. 6. (Color online) Transfer efficiency from initial $|m\rangle$ state to vibrational ground state $|g,0,0\rangle$ and back with two pulses described in Fig. 5(a). (a) The efficiency versus different laser intensity with fixed pulse length $t_p = 300\ \mu$s. (b) The round-trip efficiency as a function of laser pulse length t_p with fixed laser intensity $I_1^{\max} = 2\text{W/cm}^2$ and $I_2^{\max} = 10\text{mW/cm}^2$.

are usually tuned near resonant [73], we take the detunings $\Delta_1 \approx \Delta_2 = 2\pi \times 5$ MHz.

In Fig. 6 we investigate the round-trip transfer efficiency estimated with the parameters discussed above. An efficiency of 60% could be achieved with the best settings of laser intensity and pulse length. At low laser intensity and short pulse time region, the state transitions cannot adiabatically follow the laser pulse, which leads to low transfer efficiency. However, the increase of the laser intensity which is larger than the threshold value does not necessarily result in higher efficiency [see Fig. 6(a)], which is due to the increased decay rates induced by larger pulse intensity. To obtain the most appropriate intensity values, we test a series of maximal intensities of laser pulse $L2$ from 0.25 to 3 W/cm^2 and finally choose $I_1^{\max} = 2\text{W/cm}^2$ and $I_2^{\max} = 10\text{mW/cm}^2$ for $L1$ and $L2$, respectively. Using the optimum intensity values, the relationship between the pulse length and the transfer efficiency can be concluded from Fig. 6(b). It has the same shape with that of the efficiency versus the laser intensity and we take the optimum pulse length t_p of about 300 μs. Assuming that the round-trip STIRAP has the same efficiency for each one-way transfer and leaving out the decay of free evolution within the hold time, one-way transfer efficiency of 77% can be attained.

One thing that should be pointed out is that the purpose of the model calculations is just to make a formalistic estimation of transfer efficiency. The parameters used in the model are our reasonable assumption and should be measured in actual experiments. It is worth mentioning that the assumption may lead to underestimated efficiency. Future transferring experiments might have to resort to the vibrational state in $3(\Omega = 1/2)$ state or excited states corresponding to the $\text{Rb}(5s^2S) + \text{Sr}(5s5p^3P)$ asymptote to perform the STIRAP to achieve higher transfer efficiency.

V. CONCLUSION AND OUTLOOK

The starting point for this work is to explore the transfer scheme to produce ^{87}Rb^{84}Sr molecules in a rovibrational state. To begin with, a relativistic *ab initio* calculation with KR-MRCI approach has been performed to obtain model potentials for the ground and lowest three excited states. The results are in good agreement with recent calculated data [59].

We have also made particular investigations in detail on the rovibrational level structures and wave functions by solving the radial Schrödinger equation under a symplectic scheme with trial energy series. The number of vibrational states respectively supported by the lowest four electronic states has also been given as a prediction. However, the actual number of states should be determined by high-resolution photoassociation spectroscopy, which is currently performed by Innsbruck group [45].

Using the wave functions obtained, we have shown a full scene of the highly diagonally distributed FCFs for transitions between the rotationless ($J'' = 0$) electronic states and the excited states with $J' = 1$. Furthermore, we theoretically design a pump-dump scheme (STIRAP, Fig. 5) to transfer the formed weakly bound molecules to the rovibrational ground state with the assistance of the intermediate state $|2(\Omega = 1/2), v' = 21, J' = 1\rangle$. With reasonable assumptions and appropriate settings of laser intensity [2 W/cm^2 for $L1$ (1550 nm) laser and 10 mW/cm^2 for $L2$ (1342 nm) laser] and pulse length (about 300 μs), a round-trip transfer efficiency of 60% with one-way efficiency of 77% is predicted by the three-level model.

Since Yan *et al.* [76] have observed the Rabi oscillations between atomic and molecular condensates in a one-color photoassociation experiment for ^{88}Sr and recently Tomza *et al.* [77] have illustrated that nonresonant light can be used to control the Feshbach resonance position and width of RbYb mixtures (furthur applied to open-shell–closed-shell systems), our next goal is to investigate the dynamics of the molecular state and the approaches of controlling magnetic FRs for RbSr dimers. The results in this work pave the way for the ongoing and future experimental research on the ^{87}Rb^{84}Sr system.

ACKNOWLEDGMENTS

We would like to thank Zhenkun Chu and Deyu Li for helpful discussions on compiling and installation of the DIRAC package, and Dr. Ganesh Sashikesh for useful suggestions. The *ab initio* calculations are performed on the Magic Cube cluster (Dawning 5000A) in Shanghai Supercomputer Centre. This work is supported by the National Basic Research Program of China (Grant No. 2011CB921504) and the National Natural Science Foundation of China (Grant No. 11104292).

[1] K.-K. Ni, S. Ospelkaus, M. H. G. de Miranda, A. Pe'er, B. Neyenhuis, J. J. Zirbel, S. Kotochigova, P. S. Julienne, D. S. Jin, and J. Ye, Science **322**, 231 (2008).

[2] M. A. Baranov, M. S. Mar'enko, V. S. Rychkov, and G. V. Shlyapnikov, Phys. Rev. A **66**, 013606 (2002).

[3] K. Góral, L. Santos, and M. Lewenstein, Phys. Rev. Lett. **88**, 170406 (2002).

[4] M. A. Baranov, M. Dalmonte, G. Pupillo, and P. Zoller, Chem. Rev. **112**, 5012 (2012).

[5] E. Bodo, F. A. Gianturco, and A. Dalgarno, J. Chem. Phys. **116**, 9222 (2002).

[6] T. Zelevinsky, S. Kotochigova, and J. Ye, Phys. Rev. Lett. **100**, 043201 (2008).

[7] M. Kajita, G. Gopakumar, M. Abe, and M. Hada, Phys. Rev. A **84**, 022507 (2011).

[8] D. DeMille, Phys. Rev. Lett. **88**, 067901 (2002).

[9] A. Andre, D. DeMille, J. M. Doyle, M. D. Lukin, S. E. Maxwell, P. Rabl, R. J. Schoelkopf, and P. Zoller, Nat. Phys. **2**, 636 (2006).

[10] L. D. Carr, D. DeMille, R. V. Krems, and J. Ye, New J. Phys. **11**, 055049 (2009).

[11] J. D. Weinstein, R. deCarvalho, T. Guillet, B. Friedrich, and J. M. Doyle, Nature (London) **395**, 148 (1998).

[12] H. L. Bethlem, G. Berden, F. M. H. Crompvoets, R. T. Jongma, A. J. A. van Roij, and G. Meijer, Nature (London) **406**, 491 (2000).

[13] B. C. Sawyer, B. L. Lev, E. R. Hudson, B. K. Stuhl, M. Lara, J. L. Bohn, and J. Ye, Phys. Rev. Lett. **98**, 253002 (2007).

[14] E. S. Shuman, J. F. Barry, and D. DeMille, Nature (London) **467**, 820 (2010).

[15] D. DeMille, D. Glenn, and J. Petricka, Eur. Phys. J. D **31**, 375 (2004).

[16] G. Quemener and P. S. Julienne, Chem. Rev. **112**, 4949 (2012).

[17] S. Inouye, J. Goldwin, M. L. Olsen, C. Ticknor, J. L. Bohn, and D. S. Jin, Phys. Rev. Lett. **93**, 183201 (2004).

[18] C. A. Stan, M. W. Zwierlein, C. H. Schunck, S. M. F. Raupach, and W. Ketterle, Phys. Rev. Lett. **93**, 143001 (2004).

[19] D. A. Brue and J. M. Hutson, Phys. Rev. Lett. **108**, 043201 (2012).

[20] M. L. González-Martínez and J. M. Hutson, Phys. Rev. A **88**, 020701 (2013).

[21] M. W. Mancini, G. D. Telles, A. R. L. Caires, V. S. Bagnato, and L. G. Marcassa, Phys. Rev. Lett. **92**, 133203 (2004).

[22] C. Haimberger, J. Kleinert, M. Bhattacharya, and N. P. Bigelow, Phys. Rev. A **70**, 021402 (2004).

[23] A. J. Kerman, J. M. Sage, S. Sainis, T. Bergeman, and D. DeMille, Phys. Rev. Lett. **92**, 153001 (2004).

[24] D. Wang, J. Qi, M. F. Stone, O. Nikolayeva, H. Wang, B. Hattaway, S. D. Gensemer, P. L. Gould, E. E. Eyler, and W. C. Stwalley, Phys. Rev. Lett. **93**, 243005 (2004).

[25] N. Nemitz, F. Baumer, F. Münchow, S. Tassy, and A. Görlitz, Phys. Rev. A **79**, 061403 (2009).

[26] F. Munchow, C. Bruni, M. Madalinski, and A. Gorlitz, Phys. Chem. Chem. Phys. **13**, 18734 (2011).

[27] M. Borkowski, P. S. Żuchowski, R. Ciurylo, P. S. Julienne, D. Kedziera, L. Mentel, P. Tecmer, F. Münchow, C. Bruni, and A. Görlitz, Phys. Rev. A **88**, 052708 (2013).

[28] M. Okano, H. Hara, M. Muramatsu, K. Doi, S. Uetake, Y. Takasu, and Y. Takahashi, Appl. Phys. B **98**, 691 (2010).

[29] A. H. Hansen, A. Khramov, W. H. Dowd, A. O. Jamison, V. V. Ivanov, and S. Gupta, Phys. Rev. A **84**, 011606 (2011).

[30] H. Hara, Y. Takasu, Y. Yamaoka, J. M. Doyle, and Y. Takahashi, Phys. Rev. Lett. **106**, 205304 (2011).

[31] V. V. Ivanov, A. Khramov, A. H. Hansen, W. H. Dowd, F. Münchow, A. O. Jamison, and S. Gupta, Phys. Rev. Lett. **106**, 153201 (2011).

[32] A. H. Hansen, A. Y. Khramov, W. H. Dowd, A. O. Jamison, B. Plotkin-Swing, R. J. Roy, and S. Gupta, Phys. Rev. A **87**, 013615 (2013).

[33] S. Kato, S. Sugawa, K. Shibata, R. Yamamoto, and Y. Takahashi, Phys. Rev. Lett. **110**, 173201 (2013).

[34] A. Khramov, A. Hansen, W. Dowd, R. J. Roy, C. Makrides, A. Petrov, S. Kotochigova, and S. Gupta, Phys. Rev. Lett. **112**, 033201 (2014).

[35] K. Bergmann, H. Theuer, and B. W. Shore, Rev. Mod. Phys. **70**, 1003 (1998).

[36] S. Ospelkaus, A. Pe'er, K. K. Ni, J. J. Zirbel, B. Neyenhuis, S. Kotochigova, P. S. Julienne, J. Ye, and D. S. Jin, Nat. Phys. **4**, 622 (2008).

[37] K. Aikawa, D. Akamatsu, M. Hayashi, K. Oasa, J. Kobayashi, P. Naidon, T. Kishimoto, M. Ueda, and S. Inouye, Phys. Rev. Lett. **105**, 203001 (2010).

[38] J. M. Sage, S. Sainis, T. Bergeman, and D. DeMille, Phys. Rev. Lett. **94**, 203001 (2005).

[39] J. G. Danzl, E. Haller, M. Gustavsson, M. J. Mark, R. Hart, N. Bouloufa, O. Dulieu, H. Ritsch, and H.-C. Nagerl, Science **321**, 1062 (2008).

[40] J. G. Danzl, M. J. Mark, E. Haller, M. Gustavsson, R. Hart, J. Aldegunde, J. M. Hutson, and H.-C. Nagerl, Nat. Phys. **6**, 265 (2010).

[41] J. Kobayashi, K. Aikawa, K. Oasa, and S. Inouye, Phys. Rev. A **89**, 021401 (2014).

[42] C. P. Koch and M. Shapiro, Chem. Rev. **112**, 4928 (2012).

[43] R. Guérout, M. Aymar, and O. Dulieu, Phys. Rev. A **82**, 042508 (2010).

[44] T. Aoki, Y. Yamanaka, M. Takeuchi, Y. Torii, and Y. Sakemi, Phys. Rev. A **87**, 063426 (2013).

[45] B. Pasquiou, A. Bayerle, S. M. Tzanova, S. Stellmer, J. Szczepkowski, M. Parigger, R. Grimm, and F. Schreck, Phys. Rev. A **88**, 023601 (2013).

[46] P. S. Żuchowski, J. Aldegunde, and J. M. Hutson, Phys. Rev. Lett. **105**, 153201 (2010).

[47] S. Stellmer, B. Pasquiou, R. Grimm, and F. Schreck, Phys. Rev. Lett. **109**, 115302 (2012).

[48] L. K. Sorensen, S. Knecht, T. Fleig, and C. M. Marian, J. Phys. Chem. A **113**, 12607 (2009).

[49] W. Skomorowski, F. Pawlowski, C. P. Koch, and R. Moszynski, J. Chem. Phys. **136**, 194306 (2012).

[50] T. Fleig, J. Olsen, and L. Visscher, J. Chem. Phys. **119**, 2963 (2003).

[51] H. J. Aa. Jensen, R. Bast, T. Saue, and L. Visscher, with contributions from V. Bakken, K. G. Dyall, S. Dubillard, U. Ekström, E. Eliav, T. Enevoldsen, T. Fleig, O. Fossgaard, A. S. P. Gomes, T. Helgaker, J. K. Lærdahl, Y. S. Lee, J. Henriksson, M. Iliaš, Ch. R. Jacob, S. Knecht, S. Komorovský, O. Kullie, C. V. Larsen, H. S. Nataraj, P. Norman, G. Olejniczak, J. Olsen, Y. C. Park, J. K. Pedersen, M. Pernpointner, K. Ruud, P. Sałek, B. Schimmelpfennig, J. Sikkema, A. J. Thorvaldsen, J. Thyssen, J. van Stralen, S. Villaume, O. Visser, T. Winther, and S. Yamamoto, DIRAC, a relativistic ab initio electronic structure program, release DIRAC12, 2012 (see http://www.diracprogram.org).

[52] J. Jiang, Y. Cheng, and J. Mitroy, J. Phys. B **46**, 125004 (2013).
[53] K. G. Dyall, J. Phys. Chem. A **113**, 12638 (2009).
[54] A. S. Gomes, K. Dyall, and L. Visscher, Theor. Chem. Acc. **127**, 369 (2010).
[55] I. Angeli, At. Data Nucl. Data Tables **87**, 185 (2004).
[56] L. Visscher and K. Dyall, At. Data Nucl. Data Tables **67**, 207 (1997).
[57] S. Boys and F. Bernardi, Mol. Phys. **19**, 553 (1970).
[58] F. B. van Duijneveldt, J. G. C. M. van Duijneveldt-van de Rijdt, and J. H. van Lenthe, Chem. Rev. **94**, 1873 (1994).
[59] P. S. Żuchowski, R. Guerout, and O. Dulieu, arXiv:1402.0702 [physics.chem-ph].
[60] L. M. C. Janssen, G. C. Groenenboom, A. van der Avoird, P. S. uchowski, and R. Podeszwa, J. Chem. Phys. **131**, 224314 (2009).
[61] J. Mitroy and M. W. J. Bromley, Phys. Rev. A **68**, 052714 (2003).
[62] P. Zhang, H. R. Sadeghpour, and A. Dalgarno, J. Chem. Phys. **133**, 044306 (2010).
[63] D. A. Brue and J. M. Hutson, Phys. Rev. A **87**, 052709 (2013).
[64] S. Tohme and M. Korek, Chem. Phys. **410**, 37 (2013).
[65] R. J. LeRoy and R. B. Bernstein, J. Chem. Phys. **52**, 3869 (1970).
[66] M. Calvo and J. Sanz-Serna, *Numerical Hamiltonian Problems*, 1st ed. (Chapman and Hall, London, 1994).
[67] X.-S. Liu, X.-Y. Liu, Z.-Y. Zhou, P.-Z. Ding, and S.-F. Pan, Int. J. Quantum Chem. **79**, 343 (2000).
[68] J. Cooley, Math. Comput. **15**, 363 (1961).
[69] J. K. Cashion, J. Chem. Phys. **39**, 1872 (1963).
[70] Y. N. Martinez de Escobar, P. G. Mickelson, P. Pellegrini, S. B. Nagel, A. Traverso, M. Yan, R. Côté, and T. C. Killian, Phys. Rev. A **78**, 062708 (2008).
[71] C. Strauss, T. Takekoshi, F. Lang, K. Winkler, R. Grimm, J. Hecker Denschlag, and E. Tiemann, Phys. Rev. A **82**, 052514 (2010).
[72] K. Winkler, F. Lang, G. Thalhammer, P. v. d. Straten, R. Grimm, and J. H. Denschlag, Phys. Rev. Lett. **98**, 043201 (2007).
[73] R. Wynar, R. S. Freeland, D. J. Han, C. Ryu, and D. J. Heinzen, Science **287**, 1016 (2000).
[74] K. Winkler, G. Thalhammer, M. Theis, H. Ritsch, R. Grimm, and J. H. Denschlag, Phys. Rev. Lett. **95**, 063202 (2005).
[75] G. Reinaudi, C. B. Osborn, M. McDonald, S. Kotochigova, and T. Zelevinsky, Phys. Rev. Lett. **109**, 115303 (2012).
[76] M. Yan, B. J. DeSalvo, Y. Huang, P. Naidon, and T. C. Killian, Phys. Rev. Lett. **111**, 150402 (2013).
[77] M. Tomza, R. González-Férez, C. P. Koch, and R. Moszynski, Phys. Rev. Lett. **112**, 113201 (2014).